

Valery N. Khokhlov \* and Alexander V. Glushkov  
Odessa State Ecological University, Ukraine

## 1. INTRODUCTION

To make representation about energy balance of wave propagation in an atmosphere it is necessary to enter the intermediate characteristics determining kind of process dissipating or generating energy. This is necessary to understand the process interrelation of a various nature and different scales both in a global atmosphere and in a tropical atmosphere, in particular. As to last, the Hadley cells, synoptic eddies and moist convection exerts influence on sources and sinks of energy here.

## 2. DATA AND METHOD

The GDAAC monthly mean data set of temperature, zonal and meridional winds at 18 pressure levels from 1000 to 20 hPa for 1980-1993 period was used as initial.

The offered by Plumb (1983) energy cycle formulation, in which the energy conversions occur as  $P_E \rightarrow K_E \rightarrow K_M \rightarrow P_M$ , is assumed as a basis. Here,

$$P_E = -\frac{R}{2p} \left( \frac{p}{p_s} \right)^k \frac{\overline{\theta'^2}}{\partial \theta / \partial p}; \quad (1)$$

$$K_E = \frac{\overline{u'^2} + \overline{v'^2}}{2}; \quad (2)$$

$$K_M = \frac{\overline{u^2} + \overline{v^2}}{2}; \quad (3)$$

$$P_M = c_p \overline{T} - P_E, \quad (4)$$

$P_E$  is eddy available potential energy,  $K_E$  – eddy kinetic energy,  $K_M$  – zonal mean kinetic energy, and  $P_M$  – zonal mean potential energy. The notations in (1)-(4) are conventional and the concepts of zonal mean value and deviations from it were used:

$$\bar{f} = \frac{1}{L} \int_{-L/2}^{L/2} f dx; \quad f' = f - \bar{f},$$

where  $L$  is length of latitudinal circle.

From (4) it is shown that  $P_M$  is mainly determined by the zonal mean air temperature ( $c_p \overline{T} \gg P_E$ ) and therefore the distribution of this energy, in general, is trivial and in this work is not analyzed.

\* Corresponding author address: Valery N. Khokhlov, Odessa State Ecological Univ., Dept. of Theoretical Meteorology, Lvovskaya 15, Odessa, 65016, Ukraine; e-mail: [valerijkhokhlov@ukr.net](mailto:valerijkhokhlov@ukr.net).

The calculations were carried out for latitudinal belt between 24 S and 24 N.

## 3. RESULTS

The calculation results are shown in Figs. 1-3. In these pictures the X-axis marks correspond to the middles of a 2-degree-width latitudinal belts.

The contents of zonal mean kinetic (Fig. 1a) and eddy available potential energies (Fig. 1c) are enlarging towards the latitudinal boundary of tropical zone whereas eddy kinetic energy content (Fig. 1b) has maximum ( $0.97 \cdot 10^6 \text{ Jm}^{-2}$ ) over equator.

Such  $K_M$  distribution is assigned to the maximal values in the 200-100 hPa layer ( $23.7 \cdot 10^5 \text{ Jm}^{-2}$  at southern boundary and  $12.5 \cdot 10^5 \text{ Jm}^{-2}$  at northern one; see Fig. 2a). In the vertical structure of the  $P_E$  content there are two maximums in atmospheric boundary and 300-200 hPa layers for each hemi

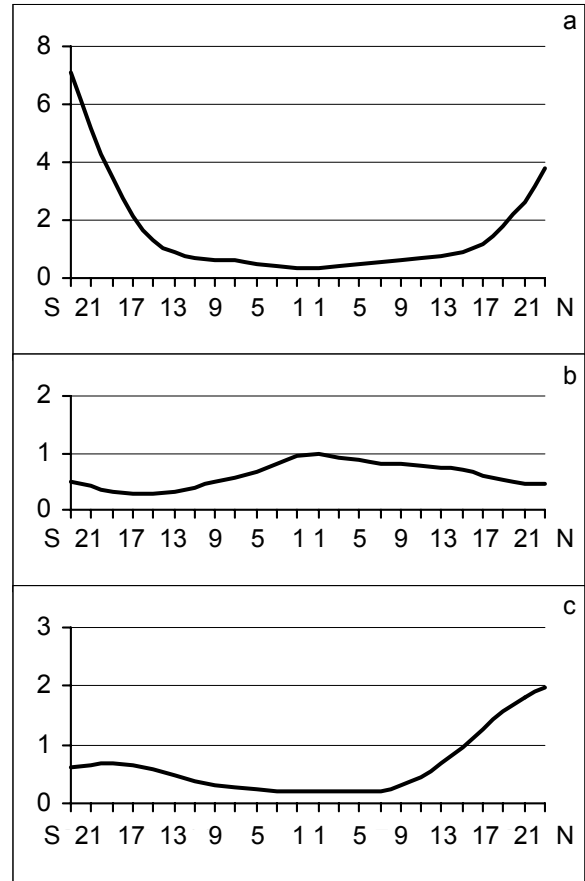


Fig. 1. Latitudinal distributions of the yearly mean content of  $K_M$  (a),  $K_E$  (b) and  $P_E$  (c) for tropics ( $\times 10^6 \text{ Jm}^{-2}$ ).

sphere (Fig. 2c). In the Southern Hemisphere these maximums are  $2.9 \cdot 10^5 \text{ J m}^{-2}$  for atmospheric boundary layer and  $1.2 \cdot 10^5 \text{ J m}^{-2}$  for top troposphere; for Northern Hemisphere they are  $4.3 \cdot 10^5 \text{ J m}^{-2}$  and  $3.4 \cdot 10^5 \text{ J m}^{-2}$  respectively. The  $K_E$  vertical structure has also two maximums over equator (Fig. 2b), first in the 800-700 hPa layer ( $1.3 \cdot 10^5 \text{ J m}^{-2}$ ) and second in the 200-100 hPa layer ( $3.1 \cdot 10^5 \text{ J m}^{-2}$ ). In this figure the Y-axis marks correspond to the middles of a 100-hPa layer.

Maximal content of  $K_M$  is registered in June ( $15.5 \cdot 10^6 \text{ J m}^{-2}$ ) at southern boundary and in February ( $17.8 \cdot 10^6 \text{ J m}^{-2}$ ) at northern one (Fig. 3a). Reverse pattern is observed for  $P_E$  spatial-time distribution (Fig. 3c). Here maximal values of  $P_E$  content are  $1.4 \cdot 10^6 \text{ J m}^{-2}$  in January at southern boundaries and  $5.4 \cdot 10^6 \text{ J m}^{-2}$  in June at northern one. Highest values of  $K_E$  content (Fig. 3b) are located on equator in January ( $1.8 \cdot 10^6 \text{ J m}^{-2}$ ) and approximately on 15 N in June ( $2.4 \cdot 10^6 \text{ J m}^{-2}$ ).

#### 4. CONCLUSIONS

The carried out analysis has shown that the energy conversion in the tropics has seasonal variability. In June-July-August the most intensive processes are realized in Southern Hemisphere and in Decem-

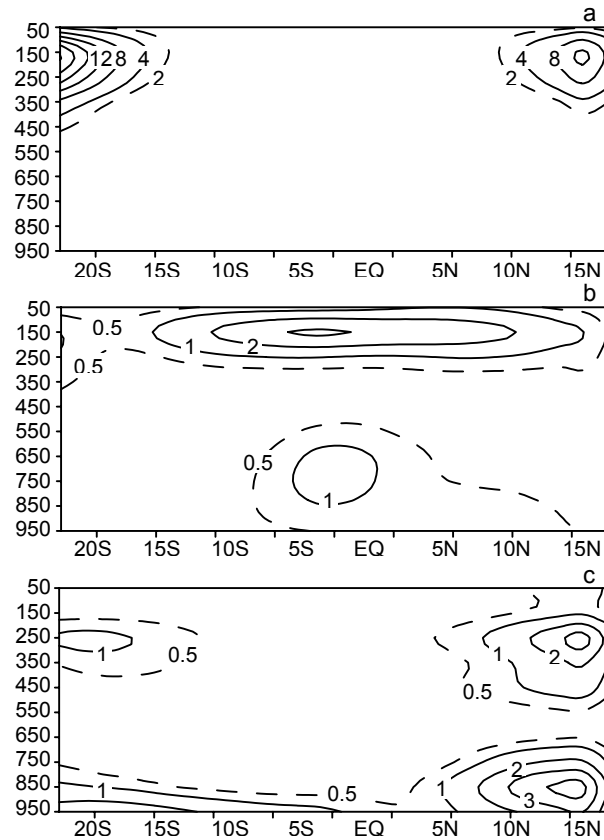


Fig. 2. Vertical cross sections of the yearly mean content of  $K_M$  (a),  $K_E$  (b) and  $P_E$  (c) for tropics ( $\times 10^5 \text{ J m}^{-2}$ ).

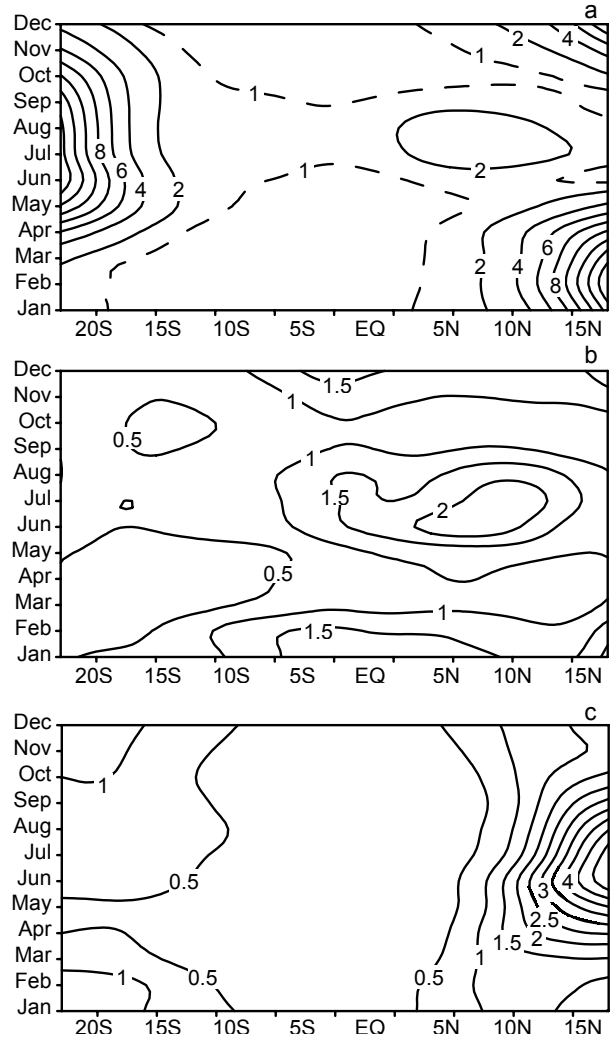


Fig. 3. Hovmöller diagrams of the yearly mean content of  $K_M$  (a),  $K_E$  (b) and  $P_E$  (c) over tropics from January to December ( $\times 10^6 \text{ J m}^{-2}$ ).

ber-January-February - in Northern Hemisphere. The available potential energy converts to the zonal mean kinetic energy and this conversion looks as decreasing of PE and increasing of KM in corresponding season. At that the intensity of Hadley cell plays the large part in this process especially in northern part of tropics. The greater heterogeneity of the terrestrial surface along latitudinal belt in Northern Hemisphere plays also the large part that consists in the conversion of eddy available potential energy into eddy kinetic one.

#### REFERENCES

Plumb, R.A., 1983: A new look at the energy cycle. *J. Atmos. Sci.*, **40**, 1669-1688.